XLVI CILAMCE
VITÓRIA - ES - BRAZIL - 2025
XLVI IBERO-LATIN AMERICAN CONGRESS ON COMPUTATIONAL METHODS IN ENGENEERING

# Application of the Virtual Element Method for two-dimensions Poisson equations

Vinícius B. A. P. Pohl[1], Marcos Arndt[1,2]

[1]*Graduate Program in Numerical Methods in Engineering, Federal University of Parana*
*81531-990, Curitiba, Parana, Brazil*
*vinicius.pohl@ufpr.br, arndt@ufpr.br*
[2]*Graduate Program in Civil Engineering, Federal University of Parana*
*81531-990, Curitiba, Parana, Brazil*

**Abstract.** The Virtual Element Method (VEM) emerges to address the need for a wide variety of non-regular polygonal meshes within a computational domain. Widely used in mathematics, physics, and engineering, the Poisson equation — a differential equation that generalizes the Laplace equation — served as one of the initial applications for the development of the Virtual Element Method. This work proposes to evaluate the performance of a two-dimensional VEM applied to the Poisson equation across different mesh types, using linear approximations. The results obtained are compared with those from the Finite Element Method (FEM), serving as a reference. The objective of this work is to assess the accuracy and convergence behavior of the method with various mesh configurations.

**Keywords:** Virtual Element Method, Finite Element Method, Poisson equation

## 1 Introduction

The Virtual Element Method is a relatively recent numerical technique, with a limited historical trajectory when compared to the Finite Element Method (FEM), which is widely recognized in the scientific and engineering literature. The Virtual Element Method (VEM) was developed as a technique for solving partial differential equations (PDEs) using a Galerkin-type approximation, while enabling the use of meshes with complex geometries. Consequently, VEM can be regarded as a generalization of the FEM.

In the early development of the Virtual Element Method (VEM), its formulation was initially applied to the Poisson equation, as demonstrated by works such as those of Da Veiga et al. [1, 2] . This equation continues to serve as a benchmark for VEM implementations, including recent studies such as those of Moherdaui and Neto [3].

This work proposes the implementation of the Virtual Element Method (VEM) for solving the Poisson equation. Its performance is compared to the standard Finite Element Method (FEM) using a linear approximation, which serves as a guideline for analyzing consistency and convergence.

The paper begins with a theoretical review of the VEM implementation procedure and its formulation in comparison to the FEM. This is followed by a discussion on the convergence behavior and an analysis of the methods' performance across a diverse set of mesh configurations.

## 2 Theoretical background

### 2.1 The Poisson equation and its variational formulation

The Poisson equation is an elliptic partial differential equation that generalizes the Laplace equation and is widely used in physics. It appears in various fields such as electromagnetism, gravitation, fluid mechanics, and heat transfer. In a domain $\Omega$, the equation takes the form:

$$-\nabla^2 u = f, \tag{1}$$

where $u$ is the potential and $f$ is the source term.

In order for the equation to be suitable for both the Finite Element Method (FEM) and the Virtual Element Method (VEM), it must be expressed in its variational form. The variational form of the Poisson equation is given by: find $u \in H^1(\Omega)$ such that for all $v \in H_0^1(\Omega)$ :

$$\int_\Omega \nabla u \nabla v \, d\Omega = \int_\Omega f v \, d\Omega, \tag{2}$$

or

$$a(u, v) = L(v) \tag{3}$$

The bilinear form $a(u, v)$ is continuous and coercive, as it has a unique solution. The proofs can be found in the works of Enabe [4] and Savarè and Chanon [5].

### 2.2 Numerical implementations

The implementation of the Virtual Element Method shares a procedure similar to that of the Finite Element Method. After the variational formulation of the partial differential equation is established, both methods follow the general steps outlined in algorithm 1.

**Algorithm 1** General implementation of the Finite Element Method and Virtual Element Method

READ MESH DATA

**for** 1 to number of elements **do**
  OBTAIN LOCAL STIFFNESS MATRIX
  OBTAIN LOCAL LOAD VECTOR

**end for**
ASSEMBLE SYSTEM OF EQUATIONS
APPLY BOUNDARY CONDITIONS
SOLVE THE SYSTEM OF EQUATION

In the Virtual Element Method (VEM), the problem domain $\Omega$ is partitioned into a polytopal mesh composed of subdomains $E$, termed elements. A polytopal mesh allows for elements with arbitrary polygonal or polyhedral shapes. The diameter of the element, denoted by $h_E$, is defined as the maximum distance between any two vertices of the element, while its area is denoted by $|E|$.

As noted in Chen and Wen [6], while FEM employs shape functions that are explicit polynomials within each element, the VEM basis functions are defined by a harmonic extension and are not explicitly known inside the element.

Given that the VEM shape functions are not explicitly known, a key feature of the Virtual Element Method is the use of a projection operator, $\Pi_{E,k}$, as highlighted by Mengolini et al. [7]. This operator maps the local VEM shape function space, $V_h(E)$, to a polynomial space, $\mathbb{P}_k(E)$, such that $\Pi_{E,k} : V_h(E) \to \mathbb{P}_k(E)$, where $k$ denotes the polynomial order.

#### Stifness matrix for the VEM

The Virtual Element Method (VEM) defines its function space, $V_{h,VEM}(E)$, in the form:

$$V_{h,VEM}(E) = \{u_h \in [H^1(E)]^2 : u_{u|e} \in \mathcal{P}_n(e) \, \forall \, e \in \partial E, \Delta u \in \mathcal{P}_{k-2}(E)\}. \tag{4}$$

This definition reveals some important properties:

- The solution $u_h$ is a polynomial of degree $k$ on each edge of the element $E$;
- It's globally continuous on the boundary $\partial E$;
- And its Laplacian, $\Delta u_h$, is a polynomial of degree $k - 2$.

While the Laplacian is the most natural choice for the Poisson equation, Da Veiga et al. [2] notes that the Laplacian operator in eq. (4) can be generalized to any second-order elliptical operator.

The degrees of freedom in the VEM are chosen to uniquely determine the solution within this space. These degrees of freedom usually include: the values of $u_h$ at the vertices; the $k-1$ internal vertices of a $(k+1)$-point Gauss-Lobatto quadrature on each edge; and its internal moments given by:

$$\frac{1}{|E|}\int_E v_h m_\alpha, \quad \alpha = 1, ..., n_{k-2}. \tag{5}$$

A central component of the VEM is the use of a Ritz projection, $\Pi^\nabla$, to connect the virtual space to a polynomial space. This projection is an elliptic operator for the Poisson problem, defined by two conditions given by:

$$\begin{cases} (\nabla(\Pi^\nabla u_h - u_h)), \nabla p_k)_{0,E} = 0 \quad \forall p \in \mathbb{P}_E \\ P_0(\Pi^\nabla u_h - u_h) = 0 \end{cases} \tag{6}$$

The first condition states that the gradient of the complement, $(\Pi^\nabla u_h - u_h)$, must be orthogonal to the gradient of any polynomial function $p_k$. Since this condition only holds up to a constant, a second operator, $P_0$, is required to ensure that the averages of the functions are equivalent.

The specific formulation of the second operator, $P_0$, depends on the order of the polynomial approximation. For the linear case, the operator is defined as the average of the function value at the element's vertices $V_i$:

$$P_0 u_h := \frac{1}{N^V}\sum_{i=1}^{N^V} u_h(V_i), \tag{7}$$

where $N^V$ is the number of vertices.

To compute the stiffness matrix in VEM, a projection of the virtual solution onto a space of explicit polynomials is required. In the VEM literature, the use of scaled monomials is a common practice, as emphasized by Moherdaui and Neto [3]. These monomials, given by:

$$m_\alpha := \left(\frac{x - x_E}{h_E}\right)^\alpha, \tag{8}$$

form a basis centered at the baricenter $(x_E, y_E)$ of the element and are scaled by it's diameter $h_E$. The set of all scaled monomials with degree less than or equal to $k$, $\mathcal{M}_k(\Omega)$, form a basis for the polynomial space $\mathcal{P}_k(E)$. As explained by Wriggers et al. [8], this formulation offers advantages in evaluating element matrices and leads to smaller conditioning values.

The Ritz projection, $\Pi^\nabla$, is defined by the orthogonality conditions given in eq. (6). As this projection maps to a polynomial space, it can be written in the scaled monomial basis, as:

$$\Pi^\nabla u_i = \sum_{\alpha=1}^{n_k} s_i^\alpha m_\alpha. \tag{9}$$

By adopting the scaled monomials as the weight function and applying them to the orthogonality relation of the gradients from eq. (6):

$$\sum_{\alpha=1}^{n_k} s_i^\alpha (\nabla m_\alpha, \nabla m_\beta)_{0,\Omega} = (\nabla m_\alpha, \nabla u_h)_{0,\Omega}. \tag{10}$$

This relationship can be expressed in matrix form as a system of equations, where the coefficient vector $s$ corresponds to the projected solution. The field variable $u_h$ is defined by its degrees of freedom through the Lagrangian identity,

$$u_h = \sum_{i=1}^{N^{dof}} \varphi_i \text{dof}_i(u_h). \tag{11}$$

where $\varphi_i$ are the shape functions and $dof_i(u_h)$ are the degrees of freedom.

By solving a system for $s$, the projection operator $\Pi_*^\nabla$ is defined in terms of the Gram matrix G of the scaled monomials and the projection matrix B, as:

$$sG = Bu_h \Rightarrow s = G^{-1}Bu_h = \Pi_*^\nabla u_h \ \therefore \ \Pi_*^\nabla = G^{-1}B. \tag{12}$$

The matrix $B$ is computated by applying the divergence theorem to the integral. This separates the integral into a boundary term and a domain term, as:

$$B = (\nabla m_\alpha, \nabla \varphi_i)_{0,\Omega} = -\int_\Omega \Delta m_\alpha \varphi_i + \int_{\partial\Omega} \frac{\partial m_\alpha}{\partial n}\varphi_i. \tag{13}$$

For a linear approximation, the domain term is null and the boundary term can be evaluated using the Gauss-Lobatto quadrature. Since the shape functions are defined as the canonical basis functions, with the property $dof_i(\varphi_j) = \delta_{i,j}$, this simplifies the matrix $B$ to the form:

$$B_{\beta,i} = \begin{Bmatrix} \frac{1}{N^V} & \dots & \frac{1}{N^V} \\ \frac{|\hat{e_1}|}{2} n_{\hat{e_1}} \cdot \nabla m_\beta & \dots & \frac{|\hat{e_N^V}|}{2} n_{\hat{e_N^V}} \cdot \nabla m_\beta \\ \frac{|\hat{e_1}|}{2} n_{\hat{e_1}} \cdot \nabla m_\beta & \dots & \frac{|\hat{e_N^V}|}{2} n_{\hat{e_N^V}} \cdot \nabla m_\beta \end{Bmatrix}, \tag{14}$$

where $\hat{e_i}$ is the line segment between the vertices $V_{i+1}$ and $V_{i-1}$ and $n_{\hat{e_i}}$ is its normal vector.

The projector $\Pi_*^\nabla$ operates on the polynomial basis. To transform it into the canonical base, a matrix $D$ is constructed, where $D_{i\alpha} = dof_i(m_\alpha)$. The final projector in the canonical basis is given by:

$$\Pi^\nabla = D\Pi_*^\nabla. \tag{15}$$

There is no need to explicitly compute the Gram matrix G through numerical integration. In the work of Da Veiga et al. [1], the authors prove an identity that simplifies the calculation of the Gram matrix $G$ in the form:

$$G = BD. \tag{16}$$

As highlighted by Manzini [9], any virtual element function can be decomposed into a polynomial part, $\Pi_k^*(V_h(E))$, and a non-polynomial part $(I - \Pi_k^*)(V_h(E))$. This decomposition of the shape function $\varphi_i$ is given by:

$$\varphi_i = \Pi^\nabla(\varphi_i) + (I - \Pi^\nabla)\varphi_i. \tag{17}$$

By substituting eq. (17) into the bilinear form $a(u, v)$ from eq. (2), the local stiffness matrix $K_{ij,VEM}$ is composed of two distinct terms: a consistency and a stability term, in the form:

$$K_{ij,VEM} = (\nabla\Pi^\nabla\varphi_i, \nabla\Pi^\nabla\varphi_j)_{0,\Omega} + (\nabla(I - \Pi^\nabla)\varphi_i, \nabla(I - \Pi^\nabla)\varphi_j)_{0,\Omega}. \tag{18}$$

The consistency term ensures that the method's behavior is accurate for polynomial solutions. This term can be computed using the Gram matrix $G$ and the projector $\Pi_*^\nabla$ as:

$$(\nabla\Pi^\nabla\varphi_i, \nabla\Pi^\nabla\varphi_j)_{0,\Omega} = \Pi_*^\nabla\tilde{G}\Pi_*^\nabla, \tag{19}$$

where $\tilde{G}$ is the $G$ matrix with its first row replaced by zeros.

The stability term ensures the method's well-posedness, even for highly distorted elements. Da Veiga et al. [2], suggests a simple but effective approximation for this term, given by:

$$\sum_{r=1}^{N^{dof}} dof_r((I - \Pi^\nabla)\varphi_i))dof_r((I - \Pi^\nabla)\varphi_j) = (I - \Pi^\nabla)^T(I - \Pi^\nabla). \tag{20}$$

By combining these two terms, the final formulation for the VEM stiffness matrix is obtained by:

$$K_{ij,VEM} = \Pi_*^\nabla\tilde{G}\Pi_*^\nabla + (I - \Pi^\nabla)^T(I - \Pi^\nabla). \tag{21}$$

**Local force vector**

The local force vector, which represents the right-hand side of the variational problem, is a crucial component for both the Finite Element and Virtual Element methods.

For the Finite Element Method, the test function $v$ on the right side of eq. (3) assumes the value of the shape function, $\varphi$. The resulting integral for a given element $E$, is:

$$F_E = \int_E f(x,y)\varphi(x,y)dE, \tag{22}$$

and can typically be evaluated using a simple one-point quadrature rule.

For the Virtual Element Method, a simplified approach is often used for linear cases. As presented by Sutton [10], the integral for the force vector can be approximated by a term that depends on the value of the source function at the element's centroid. This is represented by:

$$F_E^j = \frac{1}{|E|}\int_E \bar{\varphi_j^E}\Pi_0^E f dx \approx \frac{1}{|E|}\int_E \frac{f(x_E,y_E)}{N^V}dx = \frac{|E|}{N^V}f(x_E,y_E), \tag{23}$$

where $N^V$ is the number of vertices of the element.

This is a common and practical simplification. A similar approach to that of Sutton [10] can be seen in the work of Chen and Wen [6], which demonstrates a consistent strategy for handling the local force vector in linear VEM implementations.

## 3 Methodology

This work employs a Fortran code that implements the Virtual Element Method (VEM) for the Poisson equation. For comparison, the code also includes a standard Finite Element Method (FEM) using both linear triangle and isoparametric rectangular formulations, as detailed in Rao [11]. Both VEM and FEM are based on linear approximations for this study.

The performance of both methods is evaluated by comparing their results across different mesh patterns through the computation of the $L^2$ error. The procedures used to calculate this error are based on the work of Cangiani et al. [12].

The computational domain for this study is a unit square, denoted as $\Omega = [0,1] \times [0,1]$. Meshes with triangular and quadrilateral elements are considered for both methods, and several levels of mesh refinement are tested. The mesh patterns used for comparison, as depicted in Fig. 1 and Fig. 2, were generated using GMSH, which employs a Delaunay triangulation algorithm.

Delaunay triangulations are particularly well-suited for discretizing domains with complex geometries and generating unstructured meshes. This characteristic is crucial for a robust comparison between the Finite Element Method (FEM) and the Virtual Element Method (VEM), as it allows for an impartial assessment of their performance on non-standard and general polygonal elements, a context in which VEM is specifically designed to perform effectively.

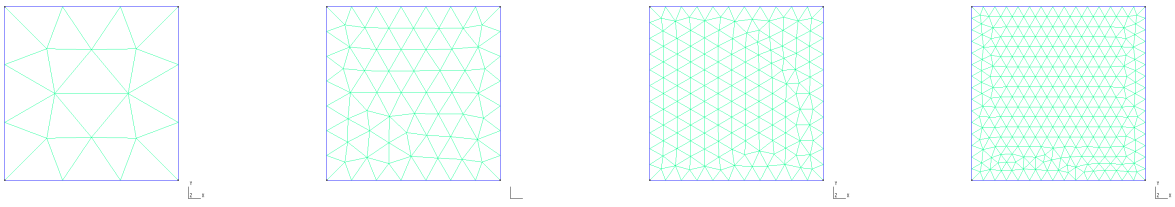

Figure 1. Triangular element meshes for the different refinement levels considered in the analysis. The total number of elements for each mesh is 26, 120, 296, and 544, respectively.

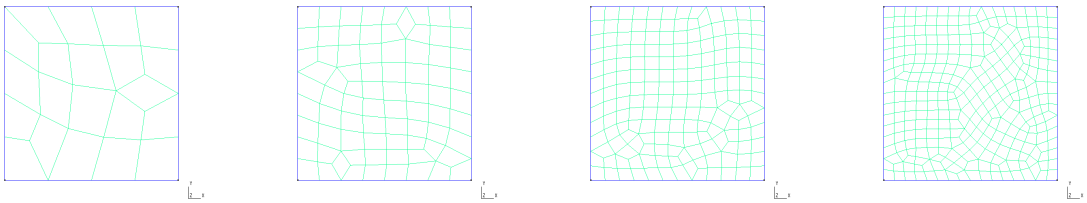

Figure 2. Quadrilateral element meshes for the different refinement levels considered in the analysis. The total number of elements for each mesh is 21, 78, 173, and 299, respectively.

The problem under analysis consists of the Poisson equation with homogeneous Dirichlet boundary conditions, ($u = 0$ on $\partial\Omega$), subjected to a source term:

$$f(x, y) = 2\pi^2 \sin(\pi x) \sin(\pi y), \tag{24}$$

with analytical solution given by:

$$u(x, y) = \sin(\pi x) \sin(\pi y) \tag{25}$$

All routines, assembly, and application of boundary conditions - except for the mesh generation - have been implemented by the authors for control and reproducibility of the analyses.

## 4 Results

This section presents the numerical results obtained from the implementation of both the Finite Element Method (FEM) and the Virtual Element Method (VEM). A convergence study was performed to assess the accuracy and behavior of the methods. Table 1 summarizes the computed $L^2$ errors for each method at various mesh sizes. These results are visually represented in Fig. 3a and Fig. 3b, which illustrates the convergence of the solutions towards the analytical solution as the mesh is progressively refined.

Table 1. $L^2$ error values for each method across various mesh refinement levels.

| h size | FEM TRI L² Error | VEM TRI L² Error | FEM QUAD L² Error | VEM QUAD L² Error |
|---|---|---|---|---|
| $2.5000E^{-1}$ | $5.4936E^{-2}$ | $9.6309E^{-2}$ | $1.6779E^{-1}$ | $3.1513E^{-1}$ |
| $1.2500E^{-1}$ | $1.1662E^{-2}$ | $2.0415E^{-2}$ | $3.0310E^{-2}$ | $1.9652E^{-2}$ |
| $8.3333E^{-2}$ | $4.7188E^{-3}$ | $8.2574E^{-3}$ | $1.4320E^{-2}$ | $8.7092E^{-3}$ |
| $6.2500E^{-2}$ | $2.5654E^{-3}$ | $4.4887E^{-3}$ | $2.3704E^{-2}$ | $5.4982E^{-3}$ |

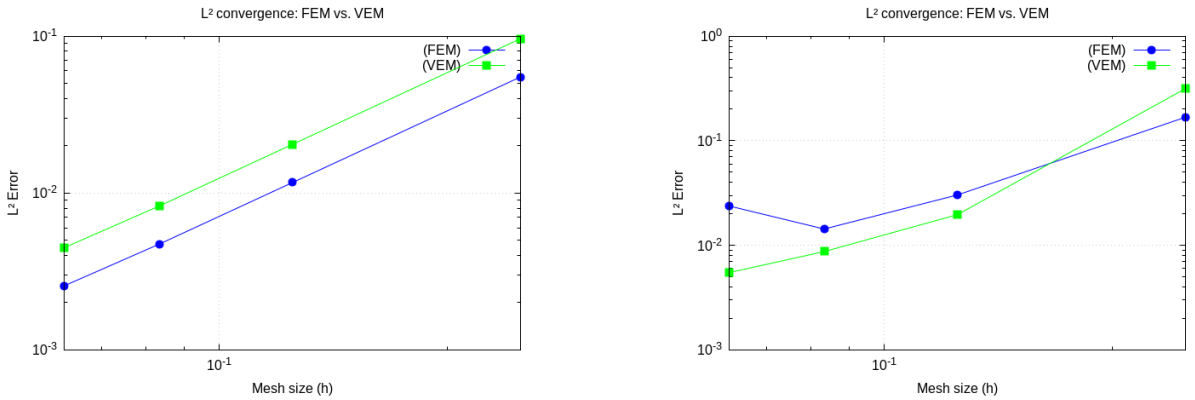


(a) Triangular elements mesh.

(b) Quadrilateral elements mesh.

Figure 3. Analysis of the convergence rate of the $L^2$ error for the implemented methods.

## 5 Conclusions

Analyzing the results obtained from the implementation, it can be observed that both the Finite Element Method (FEM) and the Virtual Element Method (VEM) demonstrate a consistent convergence rate as the element size decreases, resulting in a gradual decrease of the error. For this specific Poisson problem with triangular elements, the linear FEM solution exhibited a smaller y-intercept, as shown in Fig. 3a, indicating slightly better accuracy.

However, the convergence behavior of the two methods is different with mesh refinement for unstructured meshes with quadrilateral elements. Fig. 3b highlights that the VEM implementation initially presents a greater error than the FEM but has a more accentuated convergence slope. As the mesh is refined, the VEM's $L^2$ error, while initially larger for the 21-element quadrilateral mesh, becomes smaller than that of the FEM.

A crucial observation is the phenomenon of numerical locking, which is clearly evident in the FEM with the most refined quadrilateral mesh, see Fig. 3b. In this case, the $L^2$ error not only does not decrease but actually begins to increase. This behavior, which did not occur in the FEM when using a structured, transfinite mesh, confirms that element distortion is the root cause of the poor conditioning in the stiffness matrix, thus resulting in locking.

Under the same conditions, the VEM's $L^2$ error continues to decrease over more refined meshes. The superior performance of the VEM can be attributed to its capacity to handle elements of any polygonal shape, which effectively avoids the constraints that lead to the locking phenomenon.

**Acknowledgements** The authors acknowledge the PPGMNE (Graduate Program in Numerical Methods in Engineering) and the UFPR (Federal University of Paraná) for their institutional support. The authors gratefully acknowledge the financial support provided by CNPq (grant number: 301802/2022-0).

**Authorship statement.** The authors hereby confirm that they are the sole liable persons responsible for the authorship of this work, and that all material that has been herein included as part of the present paper is either the property (and authorship) of the authors.

## References

[1] L. B. Da Veiga, F. Brezzi, L. D. Marini, and A. Russo. The Hitchhiker's Guide to the Virtual Element Method. *Mathematical Models and Methods in Applied Sciences*, vol. 24, n. 08, pp. 1541–1573, 2014.

[2] L. B. Da Veiga, F. Brezzi, A. Cangiani, G. Manzini, L. D. Marini, and A. Russo. BASIC PRINCIPLES OF VIRTUAL ELEMENT METHODS. *Mathematical Models and Methods in Applied Sciences*, vol. 23, n. 01, pp. 199–214, 2013.

[3] T. F. Moherdaui and A. G. Neto. Virtual Element Method: An overview of formulations. *Ibero-Latin American Congress on Computational Methods in Engineering (CILAMCE)*, 2024.

[4] P. A. F. Enabe. *Virtual element method applied to the linear elastic model.* Mestrado em Engenharia de Estruturas, Universidade de São Paulo, São Paulo, 2021.

[5] S. Savarè and O. Chanon. Virtual Element Method. Master's thesis, Politecnico di Milano. Disponível em `https://github.com/deatinor/VEM3D`, 2016.

[6] L. Chen and M. Wen. Programming of linear virtual element methods. Notes. Disponível em `https://www.math.uci.edu/~chenlong/226/vemcode.pdf`, 2020.

[7] M. Mengolini, M. F. Benedetto, and A. M. Aragón. An engineering perspective to the virtual element method and its interplay with the standard finite element method. *Computer Methods in Applied Mechanics and Engineering*, vol. 350, pp. 995–1023, 2019.

[8] P. Wriggers, F. Aldakheel, and B. Hudobivnik. *Virtual Element Methods in Engineering Sciences*. Springer International Publishing, Cham, 2024.

[9] G. Manzini. Annotations on the virtual element method for second-order elliptic problems, 2016.

[10] O. J. Sutton. The virtual element method in 50 lines of MATLAB. *Numerical Algorithms*, vol. 75, n. 4, pp. 1141–1159, 2017.

[11] S. S. Rao. *The finite element method in engineering*. Butterworth-Heinemann, an imprint of Elsevier, Kidlington, Oxford, United Kingdom, sixth edition edition, 2018.

[12] A. Cangiani, E. H. Georgoulis, T. Pryer, and O. J. Sutton. A posteriori error estimates for the virtual element method. *Numerische Mathematik*, vol. 137, n. 4, pp. 857–893, 2017.